

Voltammetric Study of Two-Dimensional Phase-Transition Processes of Carboxylated Viologens at an HOPG Electrode as a Typical Organization Process of Molecules Possessing Multiple Interaction Sites

Yasuhiko Tanaka[1] **and Takamasa Sagara***[2]

[1]Department of Materials Science, Graduate School of Science and Technology, Nagasaki University, 1-14 Bunkyo, Nagasaki 852-8521

[2]Department of Applied Chemistry, Faculty of Engineering, Nagasaki University, 1-14 Bunkyo, Nagasaki 852-8521

Received November 9, 2006; E-mail: sagara@nagasaki-u.ac.jp

Two-dimensional (2D) phase-transition behavior of three different viologens, heptyl viologen and its mono- and dicarboxylated derivatives, is described using the results of voltammetric measurements at an HOPG electrode. The transition was regarded as a typical 2D molecular organization process under oxidation state control. In an acidic medium, the width of the bi-stable potential region of the phase-transition was found to increase by approximately 55 mV with each addition of a carboxylate group. This fact points to a dominant contribution from intermolecular hydrogen bonding to the reductive formation of the 2D condensed phase. The occurrence of an incomplete transition process resulting in the formation of a metastable phase at lower temperatures, higher potential sweep rates, and higher concentrations was observed for dicarboxylated viologen, but not for monocarboxylated one. These results were used to discuss the advantages and disadvantages of multiple intermolecular interaction sites in a molecule in relation to the 2D molecular organization processes.

Viologens bearing two long alkyl chains exhibit a two-dimensional (2D), first-order phase transition upon the redox reaction between a viologen dication (V^{2+}) and a radical cation ($V^{\bullet+}$) adsorbed on a basal plane of highly oriented pyrolytic graphite (HOPG),[1–6] single crystalline Au,[7–9] and Hg[10–12] electrodes. The transition takes place between a gas-like adsorption state of V^{2+} and a 2D condensed phase of $V^{\bullet+}$, accompanied by a one-electron-transfer reaction of the $V^{\bullet+/2+}$ couple. In the condensed phase on an HOPG electrode, radical cation molecules are well-aligned in a monolayer.[1,2]

We have previously reported that a dicarboxylated viologen molecule, possessing carboxylate groups at both ends of the two symmetric alkyl chains, also undergoes the phase-transition at a basal plane of an HOPG electrode.[6] Of significance is the formation of the condensed monolayer with an ordered molecular assembly of this molecule through hydrogen-bonding interaction even in an aqueous medium.

It is accepted that a prerequisite for the occurrence of the first-order phase transition is strong attractive intermolecular interaction in the condensed phase.[13–15] In the case of dicarboxylated viologen, three modes of lateral intermolecular interaction between flat-lying dicarboxylated viologen radical cation molecules should be taken into account to understand the phase-transition features, namely, π–π stacking between two $V^{\bullet+}$ moieties, interaction of alkyl chains, and the hydrogen-bonding interaction at the ends of the chains (Fig. 1). Recently, Pham and co-workers have found a stripe pattern of adsorbed $V^{\bullet+}$ form of benzyl viologen on both an HOPG and a chloride-modified Cu(100) electrode surfaces by in situ STM observations.[16] In the STM image, the main molecular axis is parallel to the surface in a side-on adsorption geometry, exhibiting the formation of π-stacked polymer chains. Figure 1 was drawn in light of their STM image in regards to the aligned pattern of $V^{\bullet+}$ moieties. When the end groups are carboxylic acid groups, direction of hydrogen-bonding may occur as an arrow c rather than c′. In the lattice gas model frequently used to describe the phase-transition, the molecules are represented by isotropic spheres.[14,17,18] The anisotropic nature of the

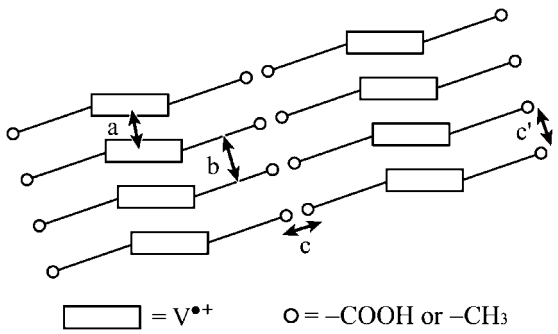

Fig. 1. Schematic depiction of the three modes of intermolecular interactions working in the 2D condensed phase of viologen radical cations on an HOPG electrode surface. Arrow a represents the π–π stacking of two $V^{\bullet+}$ moieties of side-on orientation, arrow b is the interaction of alkyl chains between the nearest neighbor molecules, arrow c is the interaction between the end groups of the alkyl chains in a longitudinal direction, and arrow c′ is the interaction between the end groups of the alkyl chains in a transverse direction.

Published on the web August 10, 2007; doi:10.1246/bcsj.80.1511

interactions between viologen radical cation molecules may provide us with an opportunity to describe the interplay of intermolecular interactions.

The phase-transition process of viologen gives rise to a spike-like cathodic peak and its counterpart anodic peak in the voltammograms at less negative potentials than the potential of the bulk redox reaction.[2] The peak separation at very slow potential sweep rates corresponds to the width of the bi-stable potential region of the phase transition.[2,6] This width can be used to give a rough estimate of the strength of the intermolecular interaction in the condensed phase.[6,19,20] The phase transition of viologens mimics an underpotential deposition (UPD) of a metal.[5] For both viologen molecules and metal ions, the lateral interaction between reduced forms in the 2D phases on an electrode substrate is so strong that very sharp voltammetric peaks are observed. In the case of an UPD, the interaction between a metal ad-atom and its neighbors is always of one kind.[21] In contrast, there are multiple interactions between a viologen radical cation molecule and its nearest neighbors, and they are anisotropic in direction and strength, as shown in Fig. 1. Therefore, the phase transition of viologen can be used to investigate the 2D organization process of organic molecules that have interaction anisotropy.

We herein describe the phase-transition behavior of an asymmetrically monocarboxylated viologen and symmetrically dicarboxylated viologen molecules in reference to the behavior of heptyl viologen (HV). In Fig. 1, both end groups represented by circles are $-CH_3$ for HV, one is $-CH_3$ and other is –COOH for monocarboxylated viologen, and both are –COOH for dicarboxylated one. Comparison of the phase-transition of these three molecules may shed light on the effect of interaction between end carboxylate groups upon the transition. Dicarboxylated viologen can form a 1D-chain linkage, while monocarboxylated viologen cannot. We therefore, focus on how the 2D condensed phase formation process is affected by whether the interaction site is at one end or the sites are at both ends.

Experimental

1,1′-Diheptyl-4,4′-bipyridinium dibromide (heptyl viologen, HV) purchased from TCI was recrystallized from water–ethanol and dried in vacuum. 1,1′-Bis(7-carboxyheptyl)-4,4′-bipyridinium dibromide (dicarboxylated viologen, V-(C_7-COOH)$_2$) was prepared previously.[6]

1-(7-Carboxyheptyl)-1′-heptyl-4,4′-bipyridinium dibromide (monocarboxylated viologen, V-C_7-COOH) was prepared by using a Menshutkin reaction between 1-heptyl-4-(4-pyridyl)pyridinium bromide and 8-bromooctanoic acid in DMF (81 °C, 24 h). Resulting precipitate was washed with acetonitrile and recrystallized from acetone–water to obtain the product as a yellow crystal (yield: 64%).

Water was purified through a Milli-Q Plus Ultrapure water system coupled with an Elix-5 kit (Millipore Co.). Its resistivity was over 18 MΩ cm. All other chemicals were of reagent grade and used as received. An HOPG plate was obtained from Matsushita Electric Co. (Panasonic graphite, PGX 04 or PGX05: size 12 × 12 × 3 mm-thickness). The graphite plate was connected perpendicularly to a copper pipe. To expose a fresh basal plane, the surface of the HOPG was peeled off using a Scotch® adhesive tape immediately before use. The HOPG electrode (electrode area: $A = 1.44\,cm^2$) was horizontally touched to the Ar gas/viologen solution interface and set in a hanging meniscus (H-M) configuration. Note that, in order for the phase transition to be realized, the setting of H-M configuration must follow the first touch of the HOPG electrode to the gas/solution interface.[2] All the electrochemical measurements were made using a Ag/AgCl/saturated KCl reference electrode and a coiled Au wire counter electrode under an Ar gas (>99.998%) atmosphere. For the voltammetric measurements, a potentiostat (HUSOU, HECS-9094) coupled with a function generator (HUSOU, HECS-321B) was employed. The function generator produces a perfectly linear potential–time relationship rather than a superposition wave of multiple small amplitude steps.

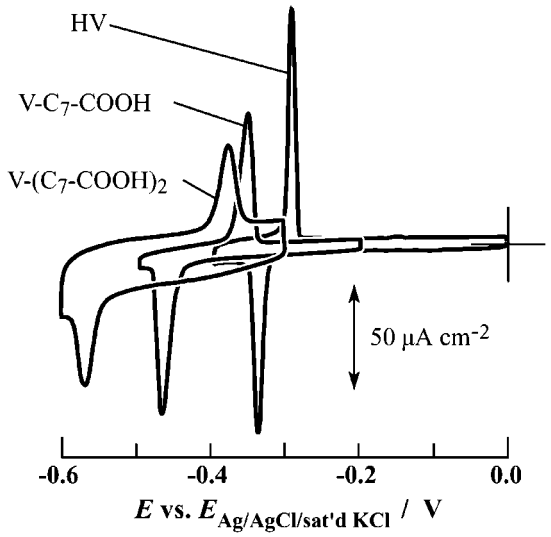

Fig. 2. Cyclic voltammograms (CVs) for HV, V-C_7-COOH, and V-(C_7-COOH)$_2$ with a sweep rate (v) of 80 mV s^{-1} in 0.3 M KBr solution 23 ± 1 °C. Solution pH was adjusted to be 2.1 by addition of HBr. Concentrations were 1.0 mM for HV and 0.1 mM for both V-C_7-COOH and V-(C_7-COOH)$_2$.

Table 1. Characteristic Potentials of CV Data for Three Different Viologens with $v = 0.4\,mV\,s^{-1}$ and $T = 23 \pm 1\,°C$

Viologen	$E_{a,1/2}$/mV	ΔE_p/mV	$\Delta(\Delta E_p)$/mV
HV	−311	12	55
V-C_7-COOH	−383	67	54
V-(C_7-COOH)$_2$	−463	121	

Results and Discussion

Voltammograms of Three Different Viologens in Acidic Medium at Room Temperature. Figure 2 shows cyclic voltammograms (CVs) for three different viologens, HV, V-C_7-COOH, and V-(C_7-COOH)$_2$, in an acidic medium at 23 ± 1 °C. All three viologens showed spike-like cathodic and anodic peaks at less-negative potentials than the potentials of the bulk redox reaction of the $V^{\bullet+/2+}$ couple. Table 1 shows the midpoint potential, $E_{a,1/2} = (E_{pa} + E_{pc})/2$, where E_{pa} is the anodic peak potential and E_{pc} is the cathodic one, and the peak separation, $\Delta E_p = E_{pa} - E_{pc}$, with a potential sweep rate (v) of 0.4 mV s^{-1}.

The negative shift in $E_{a,1/2}$ with an increase in the number of

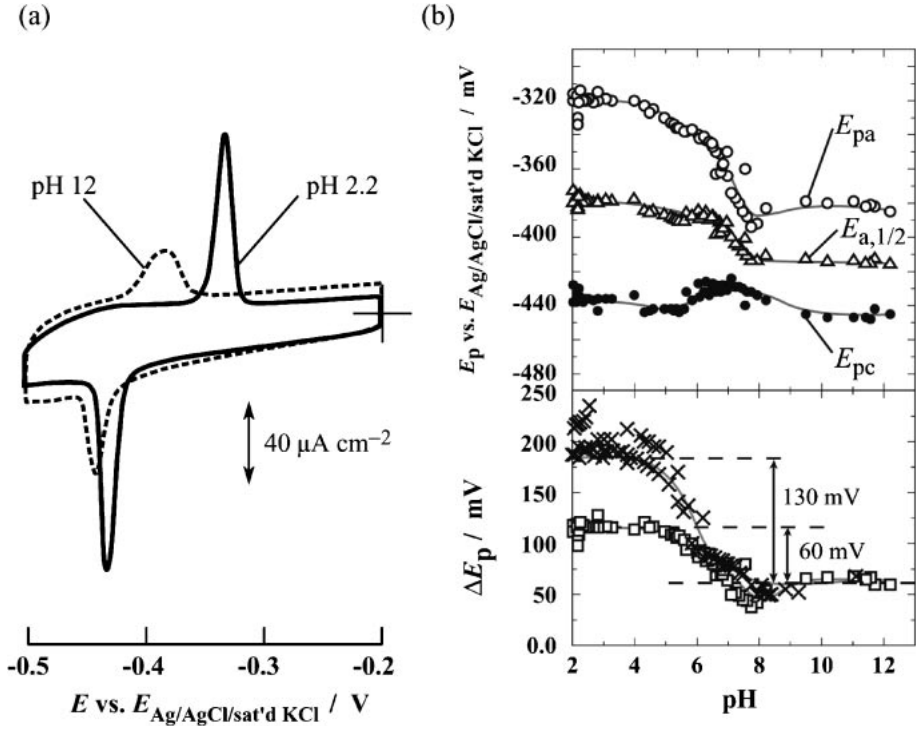

Fig. 3. (a) Comparison of CVs for V-C_7-COOH at pH 2.2 and 12 for an HOPG electrode/0.1 mM V-C_7-COOH solution with $v = 50\,\mathrm{mV\,s^{-1}}$. (b) Upper part, the plots of E_{pa}, E_{pc}, and $E_{a,1/2}$ at an HOPG electrode (Area 1.44 $\mathrm{cm^2}$) in contact with 0.1 mM V-C_7-COOH solution with $v = 50\,\mathrm{mV\,s^{-1}}$. Closed circle, E_{pc}; open circle, E_{ac}; open triangle, $E_{a,1/2}$. Lower part, the plots of ΔE_p for V-C_7-COOH and V-(C_7-COOH)$_2$. Open square, V-C_7-COOH; cross, V-(C_7-COOH)$_2$. The solid lines are added for eye-guides. Adjustment of pH was made by adding HBr, KOH, KH_2PO_4, or K_2HPO_4. Influence of phosphate ions on the CV was not observed.

carboxylic acid groups may be due to the increasing solubility of $V^{\bullet+}$ form. Because the carboxylic acid group should be desolvated as an energetically uphill process upon reductive condensation to a monolayer, the thermodynamic stability of V^{2+} relative to $V^{\bullet+}$ is higher for the species possessing more carboxylic acid groups.

We found that V-C_7-COOH also undergoes the first-order phase transition between a gas-like adsorption layer of V^{2+} form and a 2D condensed monolayer of $V^{\bullet+}$ form at the spike-like peaks, as with HV[2,4,5] and V-(C_7-COOH)$_2$.[6] This was supported by CV characteristics over a wide v-range and potential step responses (the details are not shown here but are in principle similar to those for HV and V-(C_7-COOH)$_2$). Therefore, for all three viologens in Table 1, the values of ΔE_p at very slow values of v correspond to the width of bi-stable potential region, characterizing the phase-transition behavior. The difference of ΔE_p values between V-(C_7-COOH)$_2$ and V-C_7-COOH (54 mV) was almost the same as the difference between V-C_7-COOH and HV (55 mV) (Table 1). Each addition of a carboxylic acid group increases the number of the hydrogen bonding per molecule. The contribution of the chain–chain interaction and stacking interaction between viologen radical cation moieties may remain constant. Therefore, the increase in the intermolecular interaction energy by the addition of one hydrogen bond induces a ca. 55 mV increase in the width of the bi-stable potential region.

pH Dependence of the Phase-Transition Behavior. In order for the characteristics of intermolecular interaction in the condensed monolayer of V-C_7-COOH to be clarified, the pH dependence of CV was examined in detail. Figure 3a shows typical CVs for V-C_7-COOH (0.1 mM) at two different pH values at $v = 50\,\mathrm{mV\,s^{-1}}$. In alkaline solution (pH 12), ΔE_p was smaller than that in acidic solution (pH 2.2). The carboxylic acid group is deprotonated at higher pH to afford a negatively charged carboxylate group. Deprotonation results in the loss of hydrogen-bonding ability, and simultaneously, the interaction becomes electrostatically repulsive. The attractive intermolecular interaction in the condensed monolayer is greatly weakened at higher pH, leading to the narrowing of the width of the bi-stable potential region and thus to the decrease in ΔE_p.

The upper part of Fig. 3b shows the pH dependence of the peak potentials for V-C_7-COOH with $v = 50\,\mathrm{mV\,s^{-1}}$. With an increase in the pH, a negative shift of E_a and $E_{a,1/2}$, thus a steep decrease in ΔE_p, were observed in the pH range of 4.5–8.5. This pH dependence for V-C_7-COOH followed the same trend that previously reported for V-(C_7-COOH)$_2$.[6] In the case of HV, the peak potentials were pH independent (data not shown here). The pH dependence of ΔE_p for V-C_7-COOH indicates the formation of hydrogen bonds in acidic pH region in line with V-(C_7-COOH)$_2$. The ΔE_p values for V-C_7-COOH and V-(C_7-COOH)$_2$ were almost identical in alkaline pH region, whereas they were far different in acidic pH region (lower part of Fig. 3b). The difference in ΔE_p between acidic and basic regions for V-(C_7-COOH)$_2$ was twice of that for V-C_7-COOH. This fact clearly demonstrates that the number of

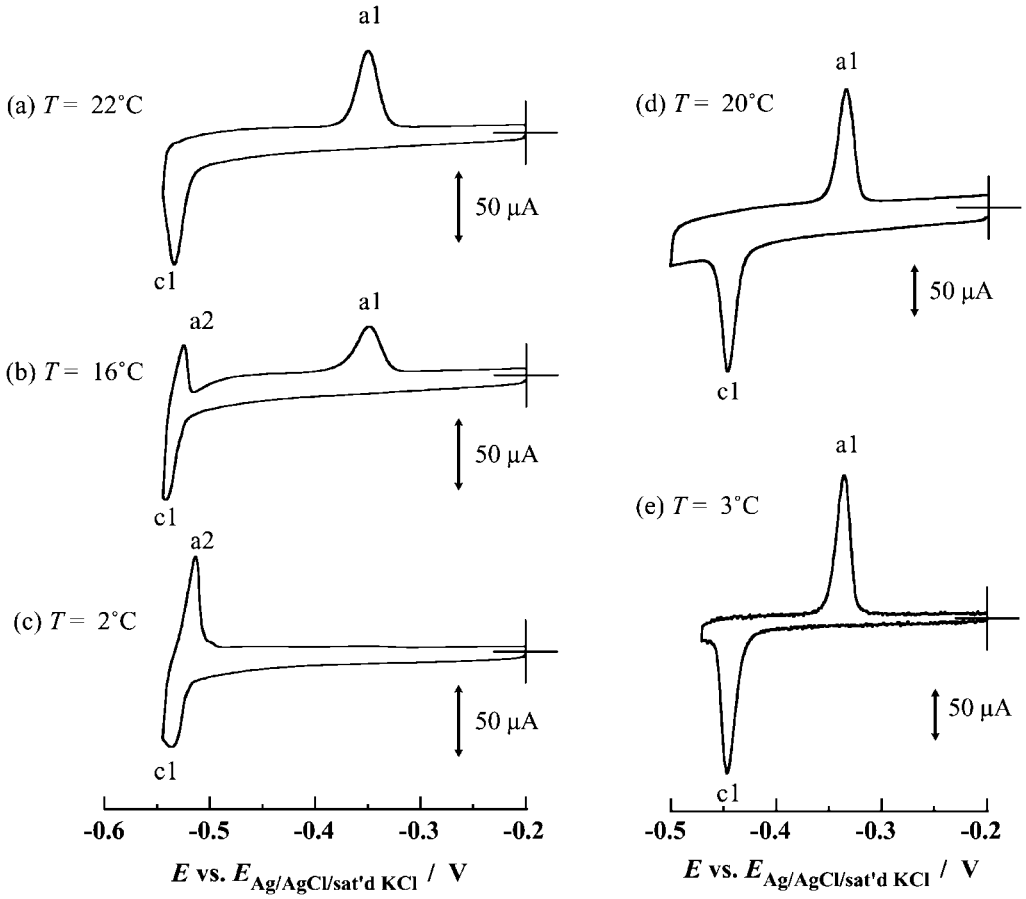

Fig. 4. (a)–(c) Typical CVs for an HOPG electrode (1.44 cm^2) in contact with 0.1 mM V-(C_7-$COOH)_2$ at pH 2.3 at three different temperatures. (d) and (e) Typical CVs for 1.0 mM V-C_7-COOH at pH 2.2 at two different temperatures. For all CVs, v = 80 mV s^{-1}.

the carboxylic acid group per viologen molecule reflects the change in ΔE_p between acidic and alkaline.

In the solution phase, the pK_a value of aliphatic carboxylic acid is around 4.8. Experimentally, the steepest shift in peak potentials occurred around pH 6.0 (lower part of Fig. 3b), a higher pH than the solution pK_a value. We have already explained this apparent pK_a shift using the results of V-(C_7-$COOH)_2$ so that the formation of hydrogen bonds as a precedent process on the HOPG basal plane surface results in the shift of the proton dissociation equilibrium of the carboxylic acid group to the alkaline direction.[6] This may also apply for V-C_7-COOH.

Effect of Temperature and Potential Sweep Rate. Although the voltammetric features and pH dependencies are in agreement for two carboxylated viologens, except for the magnitude of the peak separation, we found a drastic difference in the effects of temperature (T) and v on the CV response in an acidic medium. As described briefly in our previous paper,[6] the phase-transition behavior of V-(C_7-$COOH)_2$ is sensitive to its concentration, T, and v. Namely, irregular deposition of radical cations tends to take place when the concentration of the radical cation in close proximity of the electrode surface created at the cathodic spike-like peak is too high, T is too low, and the time period given for the alignment of the molecules on the electrode surface is too short. Fulfillment of conditions for the formation of a well-ordered 2D condensed phase of V-(C_7-$COOH)_2$ is required. In sharp contrast, such behavior was not observed for V-C_7-COOH. Note that such behavior was not observed for HV, either, at least up to 3 mM.[4]

Two carboxylated viologens were subjected to CV measurements at various T. Figure 4 shows typical CVs with v = 80 mV s^{-1}. In 0.1 mM V-(C_7-$COOH)_2$ solution, when T was lowered below 22 °C (Fig. 4b), a new anodic peak (a2) appeared at −0.53 V, and at the same time, the height of anodic peak a1 decreased. Lowering T further resulted in a gradual increase in the a2 peak height and a decrease in the a1 peak height. When T = 2 °C (Fig. 4c), peak a1 disappeared almost completely. These T dependencies for V-(C_7-$COOH)_2$ were in line with our previous results.[6] Note that the appearance and growth of peak a2 associated with the decrease and disappearance of peak a1 at low T were always observed at concentrations higher than 0.19 mM. As for V-C_7-COOH (Figs. 4d and 4e) and HV, in sharp contract, such change of CV was never observed even at a concentration as high as 1.0 mM.

In previous paper, we claimed that the condensation process of $V^{\bullet+}$-(C_7-$COOH)_2$ is sluggish.[6] When potential sweep direction was reversed at the negative vertex, irregularly deposited $V^{\bullet+}$-(C_7-$COOH)_2$ molecules remained until they are reoxidized at peak a2. The absence of peak a2 for V-C_7-COOH may indicate that $V^{\bullet+}$-C_7-COOH does not form a disordered structure.

The amount of reacted viologen molecules at each of the

Table 2. Peak Charge Values Obtained from Figs. 4a–4c

T/°C	Q_{c1}/μC	Q_{a1}/μC	Q_{a2}/μC	$(Q_{a1} + Q_{a2})$/μC
22	17.8	17.5	none	17.5
16	17.7	11.9	4.5	16.4
2	17.3	none	16.3	16.3

CV peaks is listed in Table 2 by the use of the peak charges. The peak charges for three peaks (c1, a1, and a2) were designated as Q_{c1}, Q_{a1}, and Q_{a2}, respectively. Q was obtained by integrating a plot of the voltammetric current as a function of time after background subtraction.

The value of Q_{c1} was almost constant irrespective of the appearance of peak a2. The area occupied by one $V^{\bullet+}$-$(C_7$-$COOH)_2$ molecule obtained from Q_{c1} was 130 $Å^2$/molecule. This value agrees with the calculated value of the monolayer amount of $V^{\bullet+}$-$(C_7$-$COOH)_2$ with a flat-lying adsorption orientation. The constant value of Q_{c1} indicates that, even though irregularly deposited molecules are present, a secondary overlayer is not formed. The adsorption layer structure of irregularly deposited molecules is not far different from that of a 2D condensed phase with no defects in regard to the area occupied by one molecule.

The sum of Q_{a1} and Q_{a2} was almost equal to Q_{c1} (Table 2). The reduction product at peak c1 on the electrode surface was fully reoxidized at the anodic peak(s). We also found that the position of peak a2 remained almost unchanged, whereas the Q_{a1}/Q_{a2} ratio ranged from zero to unity depending on T. Therefore, it is likely that the reduction process at peak c1 at lower T produces two distinct adsorption states of $V^{\bullet+}$-$(C_7$-$COOH)_2$. One of the states is the defect-free 2D condensed phase, and the other state gives rise to peak a2. However, an intermediate state is not produced. Although the sharpness of peak a2 indicates the presence of attractive intermolecular interaction, the peak separation between peaks c1 and a2 was much smaller than that between c1 and a1. This fact suggests that hydrogen-bonding interaction is not working effectively in the phase that gives rise to peak a2.

We also examined the potential sweep rate dependence of CV in 0.1 mM V-$(C_7$-$COOH)_2$ at 2 °C. When $v = 40\,mV\,s^{-1}$, only peak a2 was observed (Fig. 5a). When v was lowered to $16\,mV\,s^{-1}$, peak a1 was restored (Fig. 5b). When $v = 1.6\,mV\,s^{-1}$, peak a2 disappeared completely with full restoration of peak a1 (Fig. 5c). Cathodic bending distortion of the voltammetric charging current, enhanced at slower v (Fig. 5c), may be a residual current characteristic of the HOPG electrode itself.

The effect of slower potential sweep may be interpreted two ways.

(1) Formation of the ordered condensed phase occurs slowly on the HOPG surface at the cathodic peak (−0.52 V). Slower v help the formation of the ordered condensed phase with fewer defects. On the other hand, faster v allow the formation of another less-ordered condensed phase different from the ordered condensed phase. This less-ordered phase gives rise to peak a2 when it is reoxidized. These two different condensation processes take place concurrently at peak c1 at intermediate sweep rates. However, interconversion between these two different condensed phases cannot occur.

(2) Transformation of the less-ordered condensed phase of

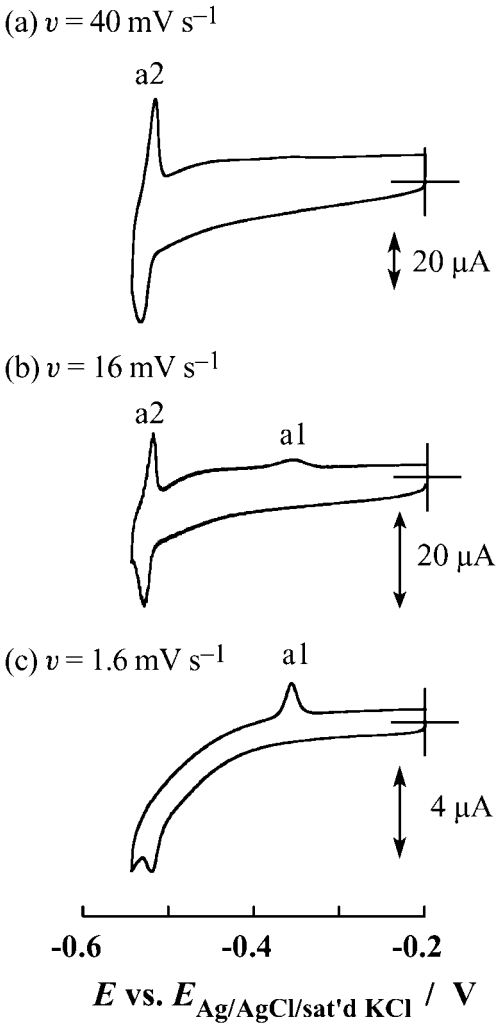

Fig. 5. CVs at three different sweep rates (v) at 2 °C for an HOPG electrode (1.44 cm^2) in contact with 0.1 mM V-$(C_7$-$COOH)_2$ solution at pH 2.3. v = (a) $40\,mV\,s^{-1}$, (b) $16\,mV\,s^{-1}$, (c) $1.6\,mV\,s^{-1}$.

$V^{\bullet+}$-forms to the ordered condensed phase is allowed in the longer time period after applying the potential of peak c1 but before the potential of peak a2. Slower v can give a longer time period. In other words, the less-ordered phase originating peak a2 is a metastable phase. The presence of the metastable phase has been found, for example, in the condensation of adenine on a Hg electrode surface.[22] It is known that, in a number of examples of the first-order phase transition of adsorbed molecules on electrode surface, the kinetics are governed in part by surface diffusion.[23–25] The transformation from the metastable phase to the ordered phase can also be governed by surface diffusion process. At lower T and faster v, however, surface diffusion is so slow that metastable phase still remains and is reoxidized at peak a2.

The latter explanation (2) means that the metastable state originating peak a2 can transform into the ordered condensed state originating peak a1. To confirm the presence of such a transformation process, potential holding experiments should be useful.

Effect of Potential Holding. To see whether a longer time

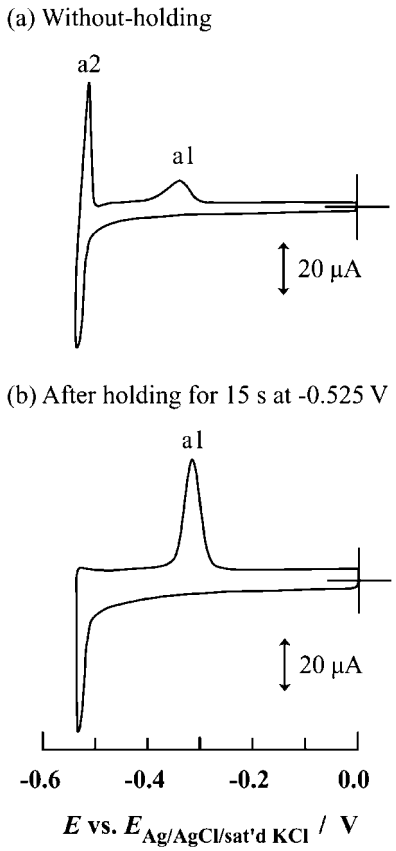

Fig. 6. Result of potential-holding experiment at 2 °C for V-(C_7-COOH)$_2$ at an HOPG electrode (1.44 cm^2) in contact with 0.1 mM V-(C_7-COOH)$_2$ solution. $v = 80\,mV\,s^{-1}$. (a) CV without holding, (b) CV after holding at −0.525 V for a period of 15 s.

period spent after the appearance of peak c1 is really effective for the restoration of peak a1 through the transformation of state, we conducted a potential holding experiment at a slightly more negative potential than that of the c1 peak. The result is demonstrated in Fig. 6. Without potential holding, peak a2 was observed at −0.50 V with the coexistence of peak a1 (Fig. 6a). When a potential holding time period of 15 s was set at the vertex potential of −0.525 V, peak a2 disappeared (Fig. 6b). Much smaller peak separation between peaks c1 and a2 than that between peaks c1 and a1 indicates that hydrogen-bonding network is ill-developed in the metastable phase. Therefore, during the holding time, radical cation molecules in the metastable phase may find their hydrogen-bonding partners. As a result, they can rearrange to an ordered state with hydrogen bonding. The transformation (reorganization) takes place from the metastable state that gives rise to peak a2 to the stable ordered condensed state that gives rise to peak a1.

Roles Played by Carboxylic Acid Group in Condensation Process. In general, a 2D phase transition is initiated with the nucleation followed by its growth. The growth process finally reaches the full monolayer condensation in an ideal case. In the case of dicarboxylated viologen, however, imperfections in the condensation process were observed at lower T and higher solution concentrations. This metastable phase gave rise to a new anodic peak a2, although this state transformed spontaneously to a regular condensed state after a certain amount of time when the potential was held at negative potentials. Since such an imperfection has not been observed for monocarboxylated viologen, the two carboxylic acid groups per molecule appears to be the cause of the imperfection.

In the growth process of the condensed phase, alignment of a molecule at the periphery of already-condensed area should occur after another.[26] This process sometimes is kinetically governed by surface diffusion.[23–25,27] As far as the acidic pH region is concerned, the diffusing species in the phase-transition of monocarboxylated viologen is either or both its monomer and hydrogen-bonded dimer. Intermolecular π–π stacking between viologen radical cation moieties may also cause the formation of another type of dimer, although we focus only on the role played by carboxylic acid group. In contrast, a variety of surface-diffusing species can be thought of for dicarboxylated viologen, including monomer, dimer, and trimer and higher oligomers as well. As described in our previous paper, hydrogen bonding on the HOPG electrode surface shifts the apparent pK_a of the carboxylic acid group.[6] This, in turn, means that surface-diffusing species includes hydrogen-bonded species before condensation.

In the case of monocarboxylated viologen, the growth process for condensation is a simple 2D "block building" process using two elemental blocks, monomer and hydrogen-bonded dimer. Thus, "mismatch" of the blocks seldom takes place. Because the largest species is just a dimer, a self-repairing process to eliminate the mismatch may be quick and easy.

In the case of dicarboxylated viologen, probability of the mismatch is rather high, and the repairing process may be complex and slow. The electrode area covered with the imperfectly condensed layer corresponds to a metastable phase. If it remains on the surface, peak a2 is observed in the CV. Because the peak separation between peaks c1 and a2 is much smaller than that between peaks c1 and a1, it is likely that hydrogen-bonding network is ill-developed in the metastable phase. Interestingly, the condensation of dicarboxylated viologen molecule of a symmetric structure is poorer at lower T than that of monocarboxylated one possessing distinct head and tail.

We can learn two important pieces of information about the nano-organization of molecules from the different behaviors of the carboxylated viologens.

(1) The increase in the number of interaction sites per molecule, thus the increase in the total attractive intermolecular interaction energy, results in the formation of an ordered and firmer molecular assembly that scarcely rearranges.

(2) The increase in the number of interaction sites results in a complex organization process as well as the production of a variety of intermediate species. Thus, too many interaction sites in a molecule sometimes interfere in the quick establishment of the defect-free molecular assembly. Then, the molecules tend to form an imperfectly ordered metastable phase.

To generalize and rationalize this concept of nano-organization of molecules, we need to follow the organization process at a molecular level and to describe the transition kinetics. The viologen phase-transition is well suited for such studies. We are currently studying the effects of stepwise addition of various interaction sites onto the viologen molecule as well as to conducting direct in situ observation of the condensation process.

Conclusion

The 2D phase-transition behavior of mono- and dicarboxylated viologens at a basal plane HOPG electrode was described in reference to the behavior of HV using cyclic voltammetry. The addition of one carboxylic acid group to HV and to monocarboxylated viologen resulted in a 55 mV increase of the width of the bi-stable potential region. The pH dependent shift of the spike-like voltammetric peak potentials of the two carboxylated viologens supported the dominant contribution of hydrogen bonding to the intermolecular interaction energy. Irregular deposition, which leads to the formation of a metastable phase, was observed for dicarboxylated viologen, but not for monocarboxylated one. Potential holding at a negative potential facilitated the spontaneous reorganization of the metastable phase to a well-ordered condensed phase.

The phase transition of viologens from gas-like adsorption layer to condensed phase can be regarded as an example of 2D nano-organization of molecules. An increase in the number of anisotropic interaction sites per molecule is advantageous for the formation of a more stable condensed phase with a wider width of the bi-stable potential region. However, it is disadvantageous for the transition process, because it slows the process and increases the chance for irregular structures.

This work is financially supported in part by the Grant-in-Aid for Scientific Research B (No. 16350077 to T.S.) from the MEXT of Japan Government. We thank Mr. T. Tada and Miss Y. Fujihara for their technical assistances.

References

1 K. Arihara, F. Kitamura, K. Nukanobu, T. Ohsaka, K. Tokuda, *J. Electroanal. Chem.* **1999**, *473*, 138.

2 T. Sagara, S. Tanaka, Y. Fukuoka, N. Nakashima, *Langmuir* **2001**, *17*, 1620.

3 T. Sagara, H. Tsuruta, Y. Fukuoka, S. Tanaka, N. Nakashima, *Studies in Surface Science and Catalysis*, ed. by Y. Iwasawa, N. Oyama, H. Kunieda, Elsevier Science B. V., **2001**, Vol. 132, p. 841.

4 T. Sagara, S. Tanaka, K. Miuchi, N. Nakashima, *J. Electroanal. Chem.* **2002**, *524–525*, 68.

5 T. Sagara, K. Miuchi, *J. Electroanal. Chem.* **2004**, *567*, 193.

6 T. Sagara, Y. Fujihara, T. Tada, *J. Electrochem. Soc.* **2005**, *152*, E239.

7 M. Tominaga, The 36th Joint Meeting of Kyushu Divisions of Chemical Societies, **1999**, Abstr., No. 4.63, p. 96.

8 K. Arihara, T. Ohsaka, F. Kitamura, *Phys. Chem. Chem. Phys.* **2002**, *4*, 1002.

9 K. Arihara, F. Kitamura, *J. Electroanal. Chem.* **2003**, *550–551*, 149.

10 J. I. Millán, R. Rodríguez-Amaro, J. J. Ruiz, L. Camacho, *J. Phys. Chem. B* **1999**, *103*, 3669.

11 K. Arihara, F. Kitamura, T. Ohsaka, K. Tokuda, *J. Electroanal. Chem.* **2000**, *488*, 117.

12 J. I. Millán, J. J. Ruiz, L. Camacho, R. Rodríguez-Amaro, *Langmuir* **2003**, *19*, 2338.

13 J. I. Millán, R. Rodríguez-Amaro, J. J. Ruiz, L. Camacho, *Langmuir* **1999**, *15*, 618.

14 T. Wandlowski, *Encyclopedia of Electrochemistry*, ed. by A. J. Bard, M. Stratmann, Wiley-VCH, Weinheim, **2003**, Vol. 1, p. 383.

15 U. Retter, H. Lohse, *J. Electroanal. Chem.* **1982**, *134*, 243.

16 D.-T. Pham, K. Gentz, C. Zörlein, N. T. H. Hai, S.-L. Tsay, B. Kirchner, S. Kossmann, K. Wandelt, P. Broekmann, *New J. Chem.* **2006**, *30*, 1439.

17 U. Retter, *J. Electroanal. Chem.* **1984**, *165*, 221.

18 Y. I. Kharkats, U. Retter, *J. Electroanal. Chem.* **1990**, *287*, 363.

19 E. Laviron, *J. Electroanal. Chem.* **1975**, *63*, 245.

20 E. Laviron, *Electroanalytical Chemistry*, ed. by A. J. Bard, Marcel Dekker, New York, **1982**, Vol. 12, p. 53.

21 F. Berthier, B. Legrand, J. Creuze, R. Tétot, *J. Electroanal. Chem.* **2004**, *561*, 37.

22 C. Prado, I. Navarro, M. Rueda, H. François, C. Buess-Herman, *J. Electroanal. Chem.* **2001**, *500*, 356.

23 U. Retter, W. Kant, *Thin Solid Films* **1995**, *256*, 89.

24 C. Donner, L. Pohlmann, H. Baumgärtel, *Surf. Sci.* **1996**, *345*, 363.

25 C. Donner, *J. Electroanal. Chem.* **2003**, *550–551*, 209.

26 N. Lin, D. Payer, A. Dmitriev, T. Strunskus, C. Wöll, J. V. Barth, K. Kern, *Angew. Chem., Int. Ed.* **2005**, *44*, 1488.

27 M. S. Maestre, R. Rodríguez-Amaro, E. Muñoz, J. J. Ruiz, L. Camacho, *J. Electroanal. Chem.* **1994**, *373*, 31.